

## Sex-specific genetic determinants of right ventricular structure and function

Lars Harbaum, MD<sup>1,2</sup>, Jan K Hennigs, MD<sup>1</sup>, Julian Pott, MD<sup>1</sup>, Jonna Ostermann, MD<sup>1</sup>, Christoph R Sinning, MD<sup>3</sup>, Arunashis Sau, MRCP<sup>2,4</sup>, Ewa Sieliwonczyk<sup>2,5,6</sup>, Fu Siong Ng, PhD<sup>2,4,7</sup>, Christopher J Rhodes, PhD<sup>2</sup>, Khodr Tello, MD<sup>8</sup>, Hans Klose, MD<sup>1</sup>, Stefan Gräf, PhD<sup>9,10</sup>, Martin R Wilkins, MD<sup>2</sup>

1. Division of Respiratory Medicine, Department of Internal Medicine II, University Medical Centre Hamburg-Eppendorf, Hamburg, Germany.
2. National Heart and Lung Institute, Faculty of Medicine, Imperial College London, London, United Kingdom.
3. Department of Cardiology, University Heart and Vascular Centre Hamburg, University Medical Centre Hamburg-Eppendorf, Member of the German Center for Cardiovascular Research (DZHK), Partner Site Hamburg/Kiel/Luebeck, Hamburg, Germany.
4. Department of Cardiology, Imperial College Healthcare NHS Trust, London, United Kingdom.
5. MRC Laboratory of Medical Sciences, Imperial College London, London, United Kingdom.
6. University of Antwerp and Antwerp University Hospital, Antwerp, Belgium.
7. Department of Cardiology, Chelsea and Westminster Hospital NHS Foundation Trust, London, United Kingdom.
8. Department of Internal Medicine, Justus-Liebig-University Giessen, Universities of Giessen and Marburg Lung Center, Member of the German Center for Lung Research (DZL), Giessen, Germany.
9. NIHR BioResource for Translational Research - Rare Diseases, Department of Haematology, University of Cambridge, Cambridge Biomedical Campus, Cambridge, United Kingdom.
10. Department of Medicine, School of Clinical Medicine, University of Cambridge, Cambridge Biomedical Campus, Cambridge, United Kingdom.

Short title: Sex-specific genetics for the right ventricle

Correspondence to: Lars Harbaum, MD, Division of Respiratory Medicine, Department of Internal Medicine II, University Medical Centre Hamburg-Eppendorf, Martinistraße 52, 20246 Hamburg, Germany. Email: [l.harbaum@uke.de](mailto:l.harbaum@uke.de). ORCID: 0000-0002-9422-6195.

The total word count of the manuscript: 7,527

## ABSTRACT

**Background:** While sex differences in right heart phenotypes have been observed, the molecular drivers remain unknown. We used common genetic variation to provide biological insights into sex differences in the structure and function of the right ventricle (RV).

**Methods:** RV phenotypes were obtained from cardiac magnetic resonance imaging in 18,156 women and 16,171 men from the UK Biobank, based on a deep-learning approach, including end-diastolic, end-systolic, and stroke volumes, as well as ejection fraction. Observational analyses and sex-stratified genome-wide association studies were performed. Candidate female-specific loci were evaluated against invasively measured hemodynamics in 479 female patients with idiopathic or heritable pulmonary arterial hypertension (PAH), recruited to the UK National Institute for Health Research BioResource Rare Diseases study.

**Results:** Sex was associated with differences in RV volumes and ejection fraction in models adjusting for left heart counterparts and lung function. Six genome-wide significant loci (13%) revealed heterogeneity of allelic effects between women and men. These included two sex-specific candidate loci present in women only; namely, a locus for RV ejection fraction in *BMPRI1A* and a locus for RV end-systolic volume near *DMRT2*. Epigenetic data indicate that variation at the *BMPRI1A* locus likely alters transcriptional regulation in RV tissue. In female patients with PAH, a variant located in the promoter of *BMPRI1A* was significantly associated with cardiac index (effect size 0.16 l/min/m<sup>2</sup>), despite similar RV afterload among genotypic groups.

**Conclusions:** We report sex-specific genetic loci for RV structure and function. *BMPRI1A* has emerged as a biologically plausible candidate gene for female-specific genetic determination of RV function, showing associations with cardiac performance under chronically increased afterload in female patients with PAH. Further studies are needed to explore the underlying biological pathways.

## ABBREVIATIONS

AMH: Anti-Müllerian hormone

BMP: Bone morphogenetic protein

BMPRI1A: Bone morphogenetic protein receptor type 1A

CMR: Cardiac magnetic resonance

DMRT2: Doublesex and mab-3 related transcription factor 2

EDV: End-diastolic volume

EF: Ejection fraction

ESV: End-systolic volume

GWAS: Genome-wide association studies

LD: Linkage disequilibrium

LSM3: Homolog, U6 small nuclear RNA and mRNA degradation associated

MAF: Minor allele frequency

NOS3: Nitric oxide synthase 3

PAH: Pulmonary arterial hypertension

QTL: Quantitative trait locus

RSRC1: Arginine and serine rich coiled-coil 1

RV: Right ventricle

SV: Stroke volume

## INTRODUCTION

Right and left heart structures are derived from different embryogenic cell populations and function under different physiological conditions.<sup>1</sup> The right ventricle (RV) is coupled to the systemic venous return and pulmonary vascular bed, coping with relatively low pre- and afterload conditions.<sup>1, 2</sup> Sex differences are common in cardiovascular physiology and diseases, and studies in populations with a low prevalence of cardiac diseases have revealed that RV volumes are smaller in women, while ejection fraction is higher compared to men.<sup>3-6</sup> In conditions primarily affecting the RV, such as pulmonary arterial hypertension (PAH), where RV failure continues to be the primary cause of mortality, sex differences in RV function and adaptation may explain the survival benefit of female patients.<sup>7-9</sup> Unravelling the molecular mechanisms underlying sex differences in RV structure and function could directly inform novel strategies to improve RV functionality and adaptation in patients with chronically increased loading conditions. Preclinical and clinical data have linked sex hormones to the difference in RV function, and the analysis of transcriptional profiles from RV tissue has observed distinct pathways associated with RV failure in women and men.<sup>10-15</sup> However, identifying these molecular mechanisms remain challenging, partly due to limited accessibility to study the human RV directly and small sample sizes.

Advances in machine learning have enabled the derivation of image-derived complex phenotypes in a manner that is scalable. This has permitted biobank-wide investigations into RV phenotypes and has revealed substantial heritability.<sup>4-6</sup> We hypothesised that, considering the moderate to high heritability, the observed sex differences in RV phenotypes may be related, in part, to genetic factors. In this report, we confirmed observational evidence indicating sex differences in RV structure and function. These findings remained consistent irrespective of left heart and lung function. Through sex-stratified genetic association testing, we identified sex-specific genetic loci in *BMPRI1A* (bone morphogenetic protein receptor type 1A) and near to *DMRT2* (doublesex and mab-3 related transcription factor 2), where associations with RV phenotypes were exclusively found in women. We prioritized the *BMPRI1A* locus based on epigenetic data in RV tissue and validated its impact on cardiac performance in female patients with PAH.

## METHODS

### *Cohort and imaging*

This research has been conducted using the UK Biobank resource, a population-based cohort that recruited individuals aged 40 – 69 years in the UK from 2006 to 2010. We analysed all participants free from a history of myocardial infarction or heart failure with available genetic and imaging data, who had not withdrawn consent as of June 2023.

Cardiac magnetic resonance (CMR) imaging was performed between 2014 and 2020 across three different assessment centres. Imaging was conducted on a clinical wide bore 1.5 Tesla scanner (MAGNETOM Aera, Syngo Platform VD13A, Siemens Healthcare, Erlangen, Germany). Three long-axis cine images and a complete stack of contiguous short-axis balanced steady state free precession cine images were captured with full biventricular coverage.<sup>16</sup> Morphology of the ventricles across a cardiac cycle were captured from segmented images based on an extensively validated deep-learning approach.<sup>4, 17</sup> Imaging phenotypes included end-diastolic volume (EDV in ml), end-systolic volume (ESV in ml), stroke volume (SV in ml) and ejection fraction (EF in %). SV and EF were calculated from EDV and ESV. We included individuals for whom all RV measurements were available.

The study protocol was approved by the Northwest Research Ethics Committee under reference number 11/NW/0382. All participants were informed and gave written informed consent. Access was provided under application number 95677.

### *Observational association*

To characterize the observational relationship between RV phenotypes and sex, generalised linear models were used in R (v4.0.3). Analyses were performed on absolute volumes and on volumes indexed for the body surface area.<sup>18</sup> RV phenotypes were the dependent variable and confounders were included as covariates. The ‘basic model’ included age, standing height, weight, waist circumference and assessment centre as covariates. In sensitivity analyses, we further adjusted for left ventricular phenotypes (‘Left heart model’) and spirometry measures (‘Lung function model’). Participants with missing covariates were excluded.

### *Genotyping, imputation and quality control.*

Genome-wide genotyping on UK Biobank participants was performed using two purpose-designed arrays (UK BiLEVE Axiom array and UK Biobank Axiom array). Imputation was performed using the Haplotype Reference Consortium and UK10K + 1000 Genomes reference panels.<sup>19</sup> Quality control measures were performed separately in women and men. We included individuals with matched self-reported and genetic sex, without evidence of sex chromosome aneuploidy, without excessive third-degree relatives, with a sample missing call rate <0.1, with a heterozygosity to missing rate within two standard deviations and with European ethnicity. We then filtered out genotyped variants with genotyping call rate <0.95 and minor allele frequency (MAF) <0.01, and imputed variants with an INFO score <0.3 and Hardy-Weinberg equilibrium exact test  $P < 1 \times 10^{-50}$ . In total, 643,281 genotyped and 9,117,541 imputed variants were included. Sex difference in allele frequencies were small (interquartile range 0.0005-0.0026)

### *Heritability and genome-wide association studies*

We conducted variance components analyses to assess heritability and genotypic correlation of RV traits using BOLT-REML (v2.4.1).<sup>20</sup> Analyses were performed separately in women, men and the sex-combined data including hard-called genotypes (all autosomes and the X-chromosome) that passed quality control in both women and men. To assess the contribution of single chromosome to

heritability, we partitioned across the chromosomes in the sex-combined dataset and repeated the analyses for each chromosome separately. Sex differences between measured heritability was assessed using Z-score and its associated P-value statistic ( $P_{\text{Heri}}$ ) as suggested previously.<sup>21</sup>

To identify single genetic variation associated with RV traits, we performed genome-wide association studies (GWAS) using BOLT-LMM (v2.4.1) which accounts for cryptic population structure and sample relatedness by fitting a linear mixed model with a Bayesian mixture prior.<sup>22</sup> We used again the full panel of hard-called genotypes to construct the genetic relationship matrix. In this analysis mode, BOLT-LMM treats individuals with one X-chromosome as having an allelic dosage of 0/2 and those with two X-chromosomes as having an allelic dosage of 0/1/2. Inverse normal transformation followed by Z-scoring was applied to the RV traits before conducting GWAS. Models were adjusted for age at recruitment, age at assessment, standing height, weight, genotype array, genotype batch, imaging centre and the first 10 principal components. Principal components were generated for each sex separately using PLINK (v2.0).<sup>23</sup> Variants at a commonly used significance threshold of  $P < 5 \times 10^{-8}$  were considered genome-wide significant. A genomic locus was defined as 5 Mb upstream and downstream of the variant with the lowest P-value. In each genomic locus, clumping for linkage disequilibrium (LD) was performed with an  $r^2$  threshold of 0.001 in the sex-combined genotypes rather than a generic reference panel.

To assess heterogeneity of GWAS loci between sexes, a fixed-effect meta-analysis framework was employed by weighting the inverse of the variance. This was performed using the '-sex' option in GWAMA (v2.2.2), which provides metrics including Cochran's Q-statistics,  $I^2$ -statistics and P-values for assessing sex-associated heterogeneity ( $P_{\text{Het}}$ ).<sup>24</sup> The effects of heterogeneous loci were categorized as sex-differential (effect in both sexes, but of different magnitude) or sex-specific (effect in one sex, but not the other), as suggested previously.<sup>21</sup> To account for possible confounding through LD, we performed statistical colocalization and tested the hypothesis of shared genetic signal (H4) using default prior probabilities as implemented in the R package coloc (v5.1.0).<sup>25</sup>

#### *Functional annotation*

Lead variants and their LD proxies ( $r^2 > 0.9$ ) were evaluated for functional consequences using the Ensembl Variant Effect Predictor tool and were assessed against publicly available epigenomic data derived from RV tissue in adult women, obtained from the ENCODE library (ENCSR821DYI, ENCSR356RNZ, ENCSR494QLL, ENCSR377RPJ) and NCBI GEO repository (GSM2322554).<sup>26-28</sup> To perform epigenetic mapping, we utilized topologically associated domains from chromatin contact maps, chromatin accessibility by DNase I hypersensitive sites and histone H3 modifications. Additionally, we investigated whether variants were associated with gene expression, employing cis-expression quantitative trait loci (QTL) in cardiac tissue from the Genotype-Tissue Expression project (GTEx v7), and performed look-ups and statistical colocalization for associations with common traits, using both GWAS catalogue and PhenoScanner (v2) databases.<sup>29-31</sup>

#### *Association with the electrocardiographic PR interval*

We evaluated candidate loci against electrocardiographic PR intervals separately for women and men, using the same study sample from the UK Biobank. All participants with available 12-lead electrocardiographic data were included. Generalized linear regression models in R were utilized, adjusting for age at assessment, standing height, weight, heart rate, electrocardiogram device, assessment centre, genotype array, genotype batch, and the first 10 principal components, as reported previously.<sup>32</sup>

#### *Association with cardiac index in pulmonary arterial hypertension*

We validated candidate loci by assessing invasively measured cardiac performance in patients with idiopathic or heritable PAH, recruited to the UK National Institute for Health Research BioResource Rare Diseases study. All enrolled patients provided written informed consent from their respective institutions. Phenotyping, genotyping, and quality control procedures were previously reported.<sup>33</sup> We included unrelated patients of European descent with available cardiac index measurements (i.e., cardiac output normalised for the body surface area, l/min/m<sup>2</sup>). Additionally, two measures of RV afterload were analysed: mean pulmonary arterial pressure (mmHg) and pulmonary vascular resistance (Wood units). Phenotypic outliers were excluded. Generalised linear regression was employed to examine single-marker variants for genetic associations with hemodynamic measures using R. Analyses were adjusted for age at diagnosis, read length chemistry, and the first 10 principal components. Principal components were again generated for each sex separately using PLINK.

## RESULTS

We investigated 18,156 women and 16,171 men of European ancestry free from pre-existing heart disease (combined 34,327 individuals). Most women (93.5%) were post-menopausal. Main characteristics of the cohort are reported in supplementary table S1.

### *Observational associations between RV phenotypes and sex*

The absolute differences in means between women and men were -47.4 ml (95% confidence interval [CI] -48.4 - -46.8) for RVEDV, -26.7 ml (95% CI -27.1 - -26.4) for RVESV, -20.6 ml (95% CI -21 - -20.3) for RVSV and 4.1 % (95% CI 4 - 4.2) for RVEF (Figure S1). Differences were similar for RV volumes indexed to the body surface area with -13.8 ml/m<sup>2</sup> (95% CI -14.1 - -13.5) for RVEDVI, -9.3 ml/m<sup>2</sup> (95% CI -9.5 - -9.1) for RVESVI and -4.5 ml/m<sup>2</sup> (95% CI -4.7 - -4.3) for RVSVI (Figure S2). Sex was independently associated with RV phenotypes in multivariable regression models accounting for left ventricular counterparts and pulmonary function. Multivariate models were adjusted for height and weight, and indexing the phenotypes to body surface area did not change results (Table 1).

Models adjusted for left ventricular phenotypes revealed the smallest effect sizes, suggesting that ventricular interdependence might partially mediate the associations. We therefore tested whether sex differences in left heart phenotypes account for the RV differences. Three RV phenotypes (RVEDV, RVESV and RVEF) remained statistically significant associated with sex after introducing the interaction term between left ventricular counterpart and sex into the model (Table S2). This suggests that while RVEDV and RVESV were smaller in women, a similar RVSV between the sexes resulted in a better RVEF in the female population.

### *Comparisons of heritability and genotypic correlations between sexes*

Structural phenotypes of RV showed substantial heritability, which was as high as 43% in women and 44% in men for RVEDV. The functional phenotype, RVEF, displayed lower heritability in both sexes (24%). Overall, there were no differences in the measured heritability between sexes ( $P_{\text{Heri}} > 0.05$ ; Figure S3). Furthermore, no individual chromosome, including the X-chromosome, contributed to the overall heritability more or less than expected given its length and number of variants (Figure S4).

Genotypic correlations were strong between RVEDV and RVSV in both women and men ( $r_g = 0.83$ ). The strongest negative correlations were observed between RVESV and RVEF, with  $r_g$  of -0.72 in women and -0.66 in men. Overall, the pattern of genotypic correlations between RV phenotypes was comparably in both sexes (Table S3).

### *Identification of individual genotypic effects*

We conducted GWAS on RV phenotypes in women, men and both sexes combined. In total, we identified 68 putative susceptibility loci at a commonly used significance threshold of  $P < 5 \times 10^{-8}$  after clumping to remove variants in LD ( $r^2 > 0.001$ ). These included 10 loci in women, 12 in men and 46 in the sex-combined analysis. Manhattan plots for all GWAS are depicted in the supplement (Figures S5 to S8). No loci were found on the X-chromosome. Multiple loci were common to both sexes, resulting in 48 unique pairs of associations between RV phenotypes and genomic regions. Similarly, several loci were shared among different RV phenotypes, and 48 unique association pairs mapped onto 28 distinct genomic regions following LD clumping across phenotypes (Table S4). In previous investigations, GWAS of RV phenotypes combining data from both sexes were conducted on the same set of CMR images, employing distinct analytical pipelines.<sup>5, 6</sup> All 48 unique pairs between RV phenotypes and genomic regions identified in the present analyses showed consistent allelic effect directions and achieved statistical significance ( $P < 0.05$ ) in at least one of the previous studies, indicating robust technical reproducibility (Table S5).



### *Identification of heterogeneity of allelic effects between sexes*

We next tested for heterogeneity of allelic effects between women and men. Among 48 unique association pairs, six pairs (13%) revealed significant heterogeneity between sexes ( $P_{\text{Het}} < 0.05$ , Figure 1A-C). These six pairs mapped to five distinct genomic regions with nearest protein-coding genes being *LSM3* (homolog, U6 small nuclear RNA and mRNA degradation associated), *RSRC1* (arginine and serine rich coiled-coil 1), *NOS3* (nitric oxide synthase 3), *DMRT2* and *BMPRI1A* (Table 2). In four association pairs, genetic effects in the sex-combined analyses were driven by one sex due to unequal effect sizes between women and men (referred to as sex-differential; Figure 1D). Stronger signals for sex-differential effects were observed in men for RVEF near *LSM3* and for RVSV and RVEDV near *NOS3*. The association between RVEF and variants in *RSRC1* showed a stronger effect in women compared to men (Table 2). At the *RSRC1* locus, lead variants with the most significant p-values were different between sexes suggesting different functional variants (posterior probability for a shared causal variant was only 1.7%; Figure S9).

We identified two association pairs that were only present in women (referred to as sex-specific; Figure 1E). Our sex-combined analyses failed to detect genome-wide significant signals at these loci (Table 3). Likewise, these loci only reached nominal significance in previous data combining sexes (Table S4). Specifically, we observed sex-specific effects in women for variants located in *BMPRI1A* on RVEF (lead variant rs111336312) and for a genomic region upstream of *DMRT2* on RVESV (lead variant rs9298673). No association signals were found at these two regions in men (Figure 2A-B).

### *Functional annotation of sex-specific loci*

The RV phenotype-associated variants at the sex-specific loci in *BMPRI1A* and near *DMRT2* were not protein-coding. We therefore searched for evidence of regulatory elements in publicly available epigenomic data from RV tissue obtained from three different adult women. Variants associated with RVEF in women extend across the introns of *BMPRI1A* and its promoter. Among these variants, rs140745739, which is highly linked to the lead variant ( $r^2 = 0.97$ ), resides directly within the promoter region, marked by a DNase I hypersensitivity indicating accessibility to the binding of transcription factors. Histone H3 lysine 4 trimethylation and lysine 27 acetylation modifications flank the promoter region, indicating active transcription (Figure 3A). In line with this, the *BMPRI1A* locus (including rs140745739) has previously been associated with significant cis-expression QTLs for *BMPRI1A* in cardiac tissue from both sexes.<sup>29</sup>

The locus that associated with RVESV in women is located within the intergenic space between *DMRT2* (the nearest gene) and *SMARCA2* (SWI/SNF related, matrix associated, actin dependent regulator of chromatin, subfamily A, member 2) and shares a topologically associated domain with both genes. Based on the available data, we did not identify evidence of an active regulatory element in RV tissue within the region containing the GWAS variants (Figure 3B).

### *Effect of BMPRI1A locus on electrocardiographic PR interval*

Annotation to common traits revealed that the *BMPRI1A* locus identified in our study colocalised with a locus for the electrocardiographic PR interval (posterior probability for a shared causal variant was 86%; Figure S10).<sup>32</sup> We subsequently assessed the association of rs140745739, located within the *BMPRI1A* promoter, with the PR interval in our study cohort. The PR interval was available for 15,287 women and 14,002 men. The minor allele C was significantly associated with a shorter PR interval in women (effect size -1.62, standard error 0.512,  $P = 0.002$ ), while no association was observed in men (effect size -0.4, standard error 0.622,  $P = 0.53$ ), emphasizing further a female-specific cardiac phenotype.

### *Effect of BMPR1A locus on cardiac performance in PAH*

PAH is characterised by chronically increased RV afterload that can compromise RVEF, followed by a reduction in cardiac index. To assess the effect of genetic variation at the *BMPR1A* locus on cardiac performance in patients with idiopathic or hereditary PAH, we correlated rs140745739 genotype with cardiac index. In 479 female patients with PAH, the minor allele C was significantly associated with an elevated cardiac index (effect size 0.16), aligning with its association with increased RVEF in UK Biobank (Figure 4A). We did not detect an association with mean pulmonary arterial pressure or pulmonary vascular resistance, indicating that the elevation in cardiac index was likely not explained by altered RV afterload. Additionally, we did not detect an effect on cardiac index in 232 male patients with PAH (effect size -0.02), despite a similar allele frequency (Table 3).

## DISCUSSION

We examined sex-stratified genetic determinants of clinically relevant RV structural and functional phenotypes derived from 34,327 CMR examinations in UK Biobank. We confirmed that women had smaller RV volumes and higher ejection fraction, which were independent of left ventricular counterparts and pulmonary function. Two sex-specific genetic associations were identified. In women, common genetic variants near the promoter of *BMPR1A*, likely affecting *BMPR1A* transcription, were identified as candidate genetic determinants of RVEF. Variants located upstream of *DMRT2* were identified as candidates influencing RVESV in women. Further investigation of female patients with PAH shows that the minor C allele at rs140745739, located in the *BMPR1A* promoter, is associated with a better cardiac index despite similar RV afterload, consistent with its association with increased RVEF in the UK Biobank cohort.

*BMPR1A* (also known as ALK3) is a biologically plausible candidate for a role in RV biology (Figure 4B). In the developing heart, *BMPR1A* is required for the expansion of the early second heart field, which subsequently contributes to growth of the RV.<sup>34</sup> During later embryogenesis, selective deletion of *BMPR1A* in cardiac myocytes results in endocardial cushion defects and myocardial thinning.<sup>35</sup> In adult mice, incomplete loss of *BMPR1A* in cardiac myocytes results in sporadically depressed RV myocardial function.<sup>36</sup> In line with these observations, rare loss-of-function mutations in *BMPR1A* have been identified in patients with congenital heart diseases.<sup>37</sup> Furthermore, *BMPR1A* signalling is required for normal AV node conduction, supporting a functional role of *BMPR1A* as a genetic determinant of the PR interval.<sup>32, 38</sup> The *BMPR1A* locus associated with RVEF in women and PR prolongation spans across the introns of *BMPR1A* and its promoter region. Epigenetic marks suggest active transcription of *BMPR1A* in RV tissue, and the location of genetic variants in the promoter region indicates a regulatory function. This interpretation is supported by the association of these variants with the *BMPR1A* transcript level in cardiac tissue.<sup>29</sup> The *BMPR1A* variants may be acting on PR interval and RVEF independently but there may also be a physiological link; longer PR intervals can have negative hemodynamic effects as a result of diastolic atrioventricular valve regurgitation, decreased ventricular preload, and a smaller SV.<sup>39-41</sup>

On a cellular level, *BMPR1A* functions as a type I receptor in the BMP signalling pathway, where it combines with the type II receptor *BMPR2* (bone morphogenetic protein receptor type 2) to bind ligands that signal through SMAD transcriptional regulators. Regulation of *BMPR1A* expression has been linked to candidate transcription factors through in silico analysis, and the rs140745739 variant is located within binding signals from ChIP-seq experiments in various cell types.<sup>28, 42</sup> The expression of *BMPR1A* is reduced in the failing RV from PAH patients, suggesting that a therapeutic strategy to increase *BMPR1A* expression would be beneficial.<sup>43</sup> Preclinical data indicate that BMP7-based small peptides, acting as activators of *BMPR1A*, might offer protection against pathological cardiac remodelling induced by pressure overload.<sup>44</sup> Additionally, *BMPR1A* has been identified as a receptor for AMH (anti-Müllerian hormone), produced by ovarian follicles in the early stages of cyclic development.<sup>45</sup> AMH has been detected in peripheral circulation, and higher levels have been linked with cardiovascular health in adult women.<sup>46</sup> Understanding cardiac BMP signalling in women could provide novel therapeutic strategies aimed at improving RV function in a group of patient that most likely to benefit from therapeutic interference.

The second sex-specific signal in women is situated in the intergenic region, between *DMRT2* and *SMARCA2*. Both genes have been implicated in organ development, but their specific roles in the cardiovascular system remain unclear. The absence of epigenetic marks in RV tissue associated with the GWAS loci emerging in our data may indeed suggest a regulatory function in non-cardiac cell systems. The *DMRT* family of genes are highly conserved transcription factors that play roles in

sexual regulation, including sex differentiation, sexual dimorphism, and spermatogenesis. *DMRT* genes are also involved in other developmental processes such as myogenesis. Notably, common genetic variants near *DMRT2* (not in LD with our GWAS variants) have been linked to skeletal muscle traits in cardiorespiratory exercise testing.<sup>47</sup> *SMARCA2* is a member of the ATP-dependent SWI/SNF complex, which modulates chromatin structure to facilitate gene transcription. Within the cardiovascular system, *SMARCA2*-mediated catalysis of the SWI/SNF complexes is required for maintaining the differentiation of vascular endothelial cells in adults.<sup>48</sup>

Several potential mechanisms may underlie genetic determinants of phenotypic differences between women and men. These mechanisms encompass the influence of sex hormones with downstream transcriptional regulation, sex-related QTL affecting both gene expression and protein expression, variations in gene splicing, and epigenetic control. Sex differences in gene expression across different tissues has been identified in around 37% of human genes.<sup>49</sup> In contrast, sex-biased cis-QTL for gene expression were less frequent but were able to inform GWAS hits, suggesting that sex-specific genetic effects on gene expression are present for a subset of previously identified cis-expression QTLs, and some of these sex-biased QTL influence genes linked to human phenotypes.<sup>49</sup>

We acknowledge limitations in our study. Our study focused on individuals of European descent and generalizability of the findings to non-European populations remains uncertain. There is overrepresentation of female participants from the UK biobank (with a ratio of 1.3:1), which may have contributed to the detection of genetic signals. Similarly, the PAH cohort was predominantly female.<sup>33</sup> Although our study provided statistical support for sex-specific loci associated with RV phenotypes, further experimental research, such as gene-editing, is required to validate our findings and annotate genetic variants with biologically meaningful functions.

In summary, our study provides observational evidence regarding the relationship between sex and RV phenotypes and evidence for sex-differences in genetic determinants, with *BMPRI1A* as a priority candidate. Performing sex-stratified genetic association analyses may contribute to our understanding of the genetic basis of phenotypic sex differences and disease outcomes. Further efforts are warranted to explore the underlying biological factors.

## ACKNOWLEDGMENT

The authors thank all volunteers and patients for their participation and acknowledge the UK Biobank and NIHR BioResource centres and staff for their contributions. We thank the NIHR BioResource – Rare Diseases Consortium and UK PAH Cohort Study Consortium as reported in <sup>33</sup> for data access. In addition, we thank Professor Renate B. Schnabel and Carla Reinbold for their review of the data presentation and statistical methods (both from the University Medical Centre Hamburg-Eppendorf).

## SOURCES OF FUNDING

The UK Biobank was established through core funding by the Wellcome Trust medical charity, the Medical Research Council, the Department of Health, the Scottish Government, and the Northwest Regional Development Agency. It has also had funding from the Welsh Government, British Heart Foundation, Cancer Research UK and Diabetes UK. This work was supported by the NIHR BioResource which supports the UK National Cohort of Idiopathic and Heritable PAH; the British Heart Foundation (BHF SP/12/12/29836) and the UK Medical Research Council (MR/K020919/1). This work was supported in part by the British Heart Foundation Centre for Research Excellence award RE/18/4/34215. Christopher J. Rhodes is supported by BHF Basic Science Research fellowship (FS/SBSRF/21/31025). Khodr Tello is supported by a German Research Foundation Collaborative Research Centre award (SFB1213/1). Arunashis Sau is supported by a British Heart Foundation clinical research training fellowship (FS/CRTF/21/24183). Ewa Sieliwonczyk is supported by a European Joint Programme on Rare Diseases research mobility fellowships (European Reference Networks). Fu Siong Ng is supported by the British Heart Foundation (RG/F/22/110078 and RE/18/4/34215) and the National Institute for Health Research Imperial Biomedical Research Centre. The funder had no role in study design, data collection, data analysis, data interpretation, or writing of this article. The views expressed are those of the authors.

## DISCLOSURES

None.

## SUPPLEMENTAL MATERIAL

This manuscript has associated supplemental tables (S1 to S5) and figures (S1 to S10).

## REFERENCES

1. Sanz J, Sánchez-Quintana D, Bossone E, Bogaard HJ, Naeije R. Anatomy, function, and dysfunction of the right ventricle: Jacc state-of-the-art review. *Journal of the American College of Cardiology*. 2019;73:1463-1482
2. Houston BA, Brittain EL, Tedford RJ. Right ventricular failure. *The New England journal of medicine*. 2023;388:1111-1125
3. Kawut SM, Lima JA, Barr RG, Chahal H, Jain A, Tandri H, et al. Sex and race differences in right ventricular structure and function: The multi-ethnic study of atherosclerosis-right ventricle study. *Circulation*. 2011;123:2542-2551
4. Bai W, Suzuki H, Huang J, Francis C, Wang S, Tarroni G, et al. A population-based phenome-wide association study of cardiac and aortic structure and function. *Nature medicine*. 2020;26:1654-1662
5. Pirruccello JP, Di Achille P, Nauffal V, Nekoui M, Friedman SF, Klarqvist MDR, et al. Genetic analysis of right heart structure and function in 40,000 people. *Nature genetics*. 2022;54:792-803
6. Aung N, Vargas JD, Yang C, Fung K, Sanghvi MM, Piechnik SK, et al. Genome-wide association analysis reveals insights into the genetic architecture of right ventricular structure and function. *Nature genetics*. 2022;54:783-791
7. Jacobs W, van de Veerdonk MC, Trip P, de Man F, Heymans MW, Marcus JT, et al. The right ventricle explains sex differences in survival in idiopathic pulmonary arterial hypertension. *Chest*. 2014;145:1230-1236
8. Swift AJ, Capener D, Hammerton C, Thomas SM, Elliot C, Condliffe R, et al. Right ventricular sex differences in patients with idiopathic pulmonary arterial hypertension characterised by magnetic resonance imaging: Pair-matched case controlled study. *PloS one*. 2015;10:e0127415
9. Tello K, Richter MJ, Yogeswaran A, Ghofrani HA, Naeije R, Vanderpool R, et al. Sex differences in right ventricular-pulmonary arterial coupling in pulmonary arterial hypertension. *American journal of respiratory and critical care medicine*. 2020;202:1042-1046
10. Ventetuolo CE, Ouyang P, Bluemke DA, Tandri H, Barr RG, Bagiella E, et al. Sex hormones are associated with right ventricular structure and function: The mesa-right ventricle study. *American journal of respiratory and critical care medicine*. 2011;183:659-667
11. Frump AL, Goss KN, Vayl A, Albrecht M, Fisher A, Tursunova R, et al. Estradiol improves right ventricular function in rats with severe angioproliferative pulmonary hypertension: Effects of endogenous and exogenous sex hormones. *American journal of physiology. Lung cellular and molecular physiology*. 2015;308:L873-890
12. Frump AL, Albrecht M, Yakubov B, Breuils-Bonnet S, Nadeau V, Tremblay E, et al. 17 $\beta$ -estradiol and estrogen receptor  $\alpha$  protect right ventricular function in pulmonary hypertension via bmpr2 and apelin. *The Journal of clinical investigation*. 2021;131
13. Liu A, Schreier D, Tian L, Eickhoff JC, Wang Z, Hacker TA, et al. Direct and indirect protection of right ventricular function by estrogen in an experimental model of pulmonary arterial hypertension. *American journal of physiology. Heart and circulatory physiology*. 2014;307:H273-283
14. Hemnes AR, Maynard KB, Champion HC, Gleaves L, Penner N, West J, et al. Testosterone negatively regulates right ventricular load stress responses in mice. *Pulmonary circulation*. 2012;2:352-358
15. Khassafi F, Chelladurai P, Valasarajan C, Nayakanti SR, Martineau S, Sommer N, et al. Transcriptional profiling unveils molecular subgroups of adaptive and maladaptive right ventricular remodeling in pulmonary hypertension. *Nature cardiovascular research*. 2023;2:917-936



16. Petersen SE, Matthews PM, Francis JM, Robson MD, Zemrak F, Boubertakh R, et al. UK biobank's cardiovascular magnetic resonance protocol. *Journal of cardiovascular magnetic resonance : official journal of the Society for Cardiovascular Magnetic Resonance*. 2016;18:8
17. Bai W, Sinclair M, Tarroni G, Oktay O, Rajchl M, Vaillant G, et al. Automated cardiovascular magnetic resonance image analysis with fully convolutional networks. *Journal of cardiovascular magnetic resonance : official journal of the Society for Cardiovascular Magnetic Resonance*. 2018;20:65
18. Mosteller RD. Simplified calculation of body-surface area. *The New England journal of medicine*. 1987;317:1098
19. Bycroft C, Freeman C, Petkova D, Band G, Elliott LT, Sharp K, et al. The uk biobank resource with deep phenotyping and genomic data. *Nature*. 2018;562:203-209
20. Loh PR, Tucker G, Bulik-Sullivan BK, Vilhjálmsson BJ, Finucane HK, Salem RM, et al. Efficient bayesian mixed-model analysis increases association power in large cohorts. *Nature genetics*. 2015;47:284-290
21. Khramtsova EA, Wilson MA, Martin J, Winham SJ, He KY, Davis LK, et al. Quality control and analytic best practices for testing genetic models of sex differences in large populations. *Cell*. 2023;186:2044-2061
22. Loh PR, Kichaev G, Gazal S, Schoech AP, Price AL. Mixed-model association for biobank-scale datasets. *Nature genetics*. 2018;50:906-908
23. Purcell S, Neale B, Todd-Brown K, Thomas L, Ferreira MA, Bender D, et al. Plink: A tool set for whole-genome association and population-based linkage analyses. *American journal of human genetics*. 2007;81:559-575
24. Magi R, Lindgren CM, Morris AP. Meta-analysis of sex-specific genome-wide association studies. *Genetic epidemiology*. 2010;34:846-853
25. Giambartolomei C, Vukcevic D, Schadt EE, Franke L, Hingorani AD, Wallace C, et al. Bayesian test for colocalisation between pairs of genetic association studies using summary statistics. *PLoS genetics*. 2014;10:e1004383
26. McLaren W, Gil L, Hunt SE, Riat HS, Ritchie GR, Thormann A, et al. The ensembl variant effect predictor. *Genome biology*. 2016;17:122
27. Schmitt AD, Hu M, Jung I, Xu Z, Qiu Y, Tan CL, et al. A compendium of chromatin contact maps reveals spatially active regions in the human genome. *Cell reports*. 2016;17:2042-2059
28. Moore JE, Purcaro MJ, Pratt HE, Epstein CB, Shores N, Adrian J, et al. Expanded encyclopaedias of DNA elements in the human and mouse genomes. *Nature*. 2020;583:699-710
29. The gtex consortium atlas of genetic regulatory effects across human tissues. *Science (New York, N.Y.)*. 2020;369:1318-1330
30. Buniello A, MacArthur JAL, Cerezo M, Harris LW, Hayhurst J, Malangone C, et al. The nhgri-ebi gwas catalog of published genome-wide association studies, targeted arrays and summary statistics 2019. *Nucleic acids research*. 2019;47:D1005-d1012
31. Staley JR, Blackshaw J, Kamat MA, Ellis S, Surendran P, Sun BB, et al. Phenoscanner: A database of human genotype-phenotype associations. *Bioinformatics (Oxford, England)*. 2016;32:3207-3209
32. Ntalla I, Weng LC, Cartwright JH, Hall AW, Sveinbjornsson G, Tucker NR, et al. Multi-ancestry gwas of the electrocardiographic pr interval identifies 202 loci underlying cardiac conduction. *Nature communications*. 2020;11:2542
33. Rhodes CJ, Batai K, Bleda M, Haimel M, Southgate L, Germain M, et al. Genetic determinants of risk in pulmonary arterial hypertension: International genome-wide association studies and meta-analysis. *The Lancet. Respiratory medicine*. 2019;7:227-238
34. Briggs LE, Phelps AL, Brown E, Kakarla J, Anderson RH, van den Hoff MJ, et al. Expression of the bmp receptor alk3 in the second heart field is essential for development of the dorsal mesenchymal protrusion and atrioventricular septation. *Circulation research*. 2013;112:1420-1432

35. Gaussin V, Van de Putte T, Mishina Y, Hanks MC, Zwijsen A, Huylebroeck D, et al. Endocardial cushion and myocardial defects after cardiac myocyte-specific conditional deletion of the bone morphogenetic protein receptor alk3. *Proceedings of the National Academy of Sciences of the United States of America*. 2002;99:2878-2883
36. El-Bizri N, Wang L, Merklinger SL, Guignabert C, Desai T, Urashima T, et al. Smooth muscle protein 22alpha-mediated patchy deletion of bmpr1a impairs cardiac contractility but protects against pulmonary vascular remodeling. *Circulation research*. 2008;102:380-388
37. D'Alessandro LC, Al Turki S, Manickaraj AK, Manase D, Mulder BJ, Bergin L, et al. Exome sequencing identifies rare variants in multiple genes in atrioventricular septal defect. *Genetics in medicine : official journal of the American College of Medical Genetics*. 2016;18:189-198
38. Stroud DM, Gaussin V, Burch JB, Yu C, Mishina Y, Schneider MD, et al. Abnormal conduction and morphology in the atrioventricular node of mice with atrioventricular canal targeted deletion of alk3/bmpr1a receptor. *Circulation*. 2007;116:2535-2543
39. Kimura Y, Fukuda K, Nakano M, Hasebe Y, Fukasawa K, Chiba T, et al. Prognostic significance of pr interval prolongation in adult patients with total correction of tetralogy of fallot. *Circulation. Arrhythmia and electrophysiology*. 2018;11:e006234
40. Salden F, Kutuyifa V, Stockburger M, Prinzen FW, Vernooy K. Atrioventricular dromotopathy: Evidence for a distinctive entity in heart failure with prolonged pr interval? *Europace : European pacing, arrhythmias, and cardiac electrophysiology : journal of the working groups on cardiac pacing, arrhythmias, and cardiac cellular electrophysiology of the European Society of Cardiology*. 2018;20:1067-1077
41. Barold SS, Ilercil A, Leonelli F, Herweg B. First-degree atrioventricular block. Clinical manifestations, indications for pacing, pacemaker management & consequences during cardiac resynchronization. *Journal of interventional cardiac electrophysiology : an international journal of arrhythmias and pacing*. 2006;17:139-152
42. Dahdaleh FS, Carr JC, Calva D, Howe JR, Howe JR. Sp1 regulates the transcription of bmpr1a. *The Journal of surgical research*. 2011;171:e15-20
43. Boucherat O, Yokokawa T, Krishna V, Kalyana-Sundaram S, Martineau S, Breuils-Bonnet S, et al. Identification of Itbp-2 as a plasma biomarker for right ventricular dysfunction in human pulmonary arterial hypertension. *Nature cardiovascular research*. 2022;1:748-760
44. Salido-Medina AB, Gil A, Expósito V, Martínez F, Redondo JM, Hurlé MA, et al. Bmp7-based peptide agonists of bmpr1a protect the left ventricle against pathological remodeling induced by pressure overload. *Biomedicine & pharmacotherapy = Biomedecine & pharmacotherapie*. 2022;149:112910
45. Jamin SP, Arango NA, Mishina Y, Hanks MC, Behringer RR. Requirement of bmpr1a for müllerian duct regression during male sexual development. *Nature genetics*. 2002;32:408-410
46. de Kat AC, Verschuren WM, Eijkemans MJ, Broekmans FJ, van der Schouw YT. Anti-müllerian hormone trajectories are associated with cardiovascular disease in women: Results from the doetinchem cohort study. *Circulation*. 2017;135:556-565
47. Ghosh S, Hota M, Chai X, Kiranya J, Ghosh P, He Z, et al. Exploring the underlying biology of intrinsic cardiorespiratory fitness through integrative analysis of genomic variants and muscle gene expression profiling. *Journal of applied physiology (Bethesda, Md. : 1985)*. 2019;126:1292-1314
48. Willis MS, Homeister JW, Rosson GB, Annayev Y, Holley D, Holly SP, et al. Functional redundancy of swi/snf catalytic subunits in maintaining vascular endothelial cells in the adult heart. *Circulation research*. 2012;111:e111-122
49. Oliva M, Muñoz-Aguirre M, Kim-Hellmuth S, Wucher V, Gewirtz ADH, Cotter DJ, et al. The impact of sex on gene expression across human tissues. *Science (New York, N.Y.)*. 2020;369



**Table 1:** Effect estimates of female sex on right ventricular (RV) imaging traits in multivariable linear regression models.

Phenotype	Unit*	Basic model <sup>†</sup>			Left heart model <sup>‡</sup>			Lung function model <sup>§</sup>		
		$\beta$	95% CI	P	$\beta$	95% CI	P	$\beta$	95% CI	P
RVEDV	ml	-27.8	-28.6 - -26.9	<0.001	-11.5	-12 - -10.9	<0.001	-24.8	-25.7 - -23.8	<0.001
	ml/m <sup>2</sup>	-14.5	-14.9 - -14.1	<0.001	-6.1	-6.4 - -5.8	<0.001	-13.1	-13.5 - -12.6	<0.001
RVESV	ml	-17.3	-17.8 - -16.8	<0.001	-9.4	-9.8 - -9	<0.001	-16.1	-16.7 - -15.6	<0.001
	ml/m <sup>2</sup>	-9.1	-9.3 - -8.8	<0.001	-4.9	-5.1 - -4.7	<0.001	-8.5	-8.8 - -8.2	<0.001
RVSV	ml	-10.5	-11 - -9.9	<0.001	-4.2	-4.5 - -3.8	<0.001	-8.6	-9.2 - -8	<0.001
	ml/m <sup>2</sup>	-5.4	-5.7 - -5.2	<0.001	-2.2	-2.4 - -2	<0.001	-4.5	-4.8 - -4.2	<0.001
RVEF	%	3.4	3.2 - 3.6	<0.001	2	1.8 - 2.2	<0.001	3.5	3.3 - 3.8	<0.001

\* RV volumes were assessed as either absolute measures in ml or indexed for the body surface area in ml/m<sup>2</sup>.

<sup>†</sup> Basic model includes age, standing height, weight, waist circumference and assessment centre.

<sup>‡</sup> Left heart model includes the basic model and the LV counterpart (LVEDV, LVESV, LVSV or LVEF; either as absolute value of or indexed for the body surface area).

<sup>§</sup> Lung function model includes the basic model and spirometry (FEV1, FVC and FEV1 to FVC ratio).

Confidence interval (CI). Forced expiratory volume in 1 second (FEV1). Forced vital capacity (FVC). Left ventricle (LV). LV end-diastolic volume (LVEDV). LV end-systolic volume (LVESV). LV stroke volume (LVSV). LV ejection fraction (LVEF). RV end-diastolic volume (RVEDV). RV end-systolic volume (RVESV). RV stroke volume (RVSV). RV ejection fraction (RVEF).

**Table 2:** Genetic loci with heterogeneous effects between women and men on right ventricular (RV) phenotypes.

	Locus and lead variant			Sex-stratified association						Sex-combined association			Heterogeneity		
				Women			Men			EAF	BETA (SE)	P	Q	I <sup>2</sup>	P <sub>Het</sub>
	Gene	Variant	EA	EAF	BETA (SE)	P	EAF	BETA (SE)	P						
Sex-specific effects															
RVESV	<i>DMRT2</i>	rs9298673	C	0.77	0.06 (0.011)	2 x10 <sup>-8</sup>	0.77	0.01 (0.012)	0.28	0.77	0.03 (0.006)	1.7 x10 <sup>-6</sup>	9	0.89	0.003
RVEF	<i>BMPR1A</i>	rs111336312	GA	0.08	0.11 (0.019)	4.7 x10 <sup>-8</sup>	0.08	0.01 (0.02)	0.45	0.08	0.06 (0.013)	1.6 x10 <sup>-5</sup>	10.6	0.91	0.001
Sex-differential effects															
RVEF	<i>LSM3</i>	rs55834511	C	0.22	-0.04 (0.013)	0.003	0.21	-0.1 (0.013)	6.8 x10 <sup>-14</sup>	0.22	-0.06 (0.009)	2.5 x10 <sup>-13</sup>	11.6	0.91	<0.001
RVEF*	<i>RSRC1</i>	rs9865460	A	0.47	-0.06 (0.01)	1.2 x10 <sup>-9</sup>	0.47	-0.01 (0.011)	0.25	0.47	-0.04 (0.007)	1.1 x10 <sup>-7</sup>	11.1	0.91	<0.001
		rs3851363	A	0.52	-0.05 (0.01)	7 x10 <sup>-7</sup>	0.52	-0.03 (0.01)	0.003	0.52	-0.04 (0.007)	1.2 x10 <sup>-8</sup>	-	-	-
RVSV	<i>NOS3</i>	rs3918226	T	0.08	-0.03 (0.017)	0.07	0.08	-0.12 (0.019)	1.1 x10 <sup>-9</sup>	0.08	-0.06 (0.011)	3 x10 <sup>-8</sup>	10.8	0.91	0.001
RVEDV					-0.04 (0.016)	0.03		-0.11 (0.018)	2.1 x10 <sup>-9</sup>		-0.05 (0.01)	2.5 x10 <sup>-8</sup>			

\* Sexes showed distinct lead variants (the variant with the most significant p-value) at this locus. In women, the lead variant (rs9865460) displayed the most significant p-value among all sexes and was found to be in linkage disequilibrium ( $r^2=0.36$ ) with the lead variants observed in men and in the combined analysis (rs3851363).

Bone morphogenetic protein receptor type 1A (*BMPR1A*). Doublesex and mab-3 related transcription factor 2 (*DMRT2*). Effect allele (EA). Effect allele frequency (EAF). Homolog, U6 small nuclear RNA and mRNA degradation associated (*LSM3*). Nitric oxide synthase 3 (*NOS3*). Arginine and serine rich coiled-coil 1(*RSRC1*). RV end-diastolic volume (RVEDV). RV end-systolic volume (RVESV). RV stroke volume (RVSV). RV ejection fraction (RVEF). Standard error (SE).

**Table 3:** Genotypic effect of each minor allele C at rs140745739 on hemodynamic measures in patients with idiopathic or hereditary pulmonary arterial hypertension (PAH).

Sex	Phenotype	Unit	N	EAF	BETA (SE)	P	
Women	Cardiac index	l/min/m <sup>2</sup>	479	0.07	0.16 (0.076)	0.04	
	RV afterload	mPAP	mmHg	545	0.07	-1.03 (1.42)	0.47
		PVR	WU	461	0.08	-0.04 (0.644)	0.94
Men*	Cardiac index	l/min/m <sup>2</sup>	232	0.07	-0.02 (0.139)	0.87	

\* The frequencies of the minor allele C were comparable between female and male patients; however, as expected in the smaller sample size, no male patients were homozygous for the minor allele.

Effect allele frequency (EAF). Mean pulmonary arterial pressure (mPAP). Pulmonary vascular resistance (PVR). Standard error (SE). Wood units (WU).

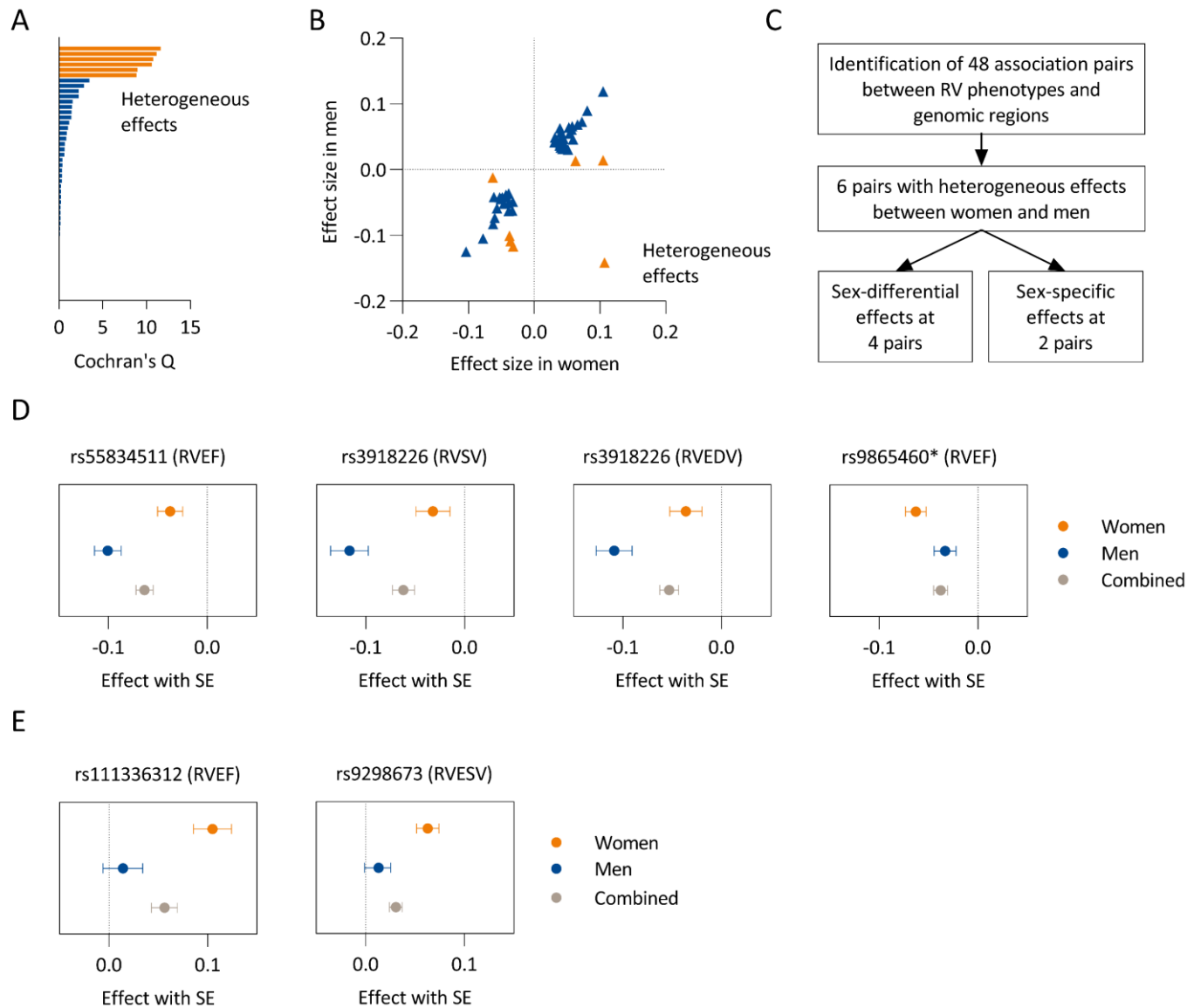


**Figure 1:** Heterogeneity in allelic effects between women and men.

In **A** and **B**, six association pairs were highlighted that showed significant heterogeneity between women and men. The effects of these six association pairs were distinguished into four sex-differential effects, where the combined effect was predominantly driven by one sex, and two sex-specific effects, which were present in only one sex (**C**). Sex-differential allelic effects are depicted in **D** and sex-specific effects in **E**. The asterisk indicate that in men rs3851363 ( $r^2$  0.36 with lead variant in women) was used due to signal differences between women and men.

Right ventricle (RV). RV end-diastolic volume (RVEDV). RV end-systolic volume (RVESV). RV stroke volume (RVSV). RV ejection fraction (RVEF). Standard error (SE).

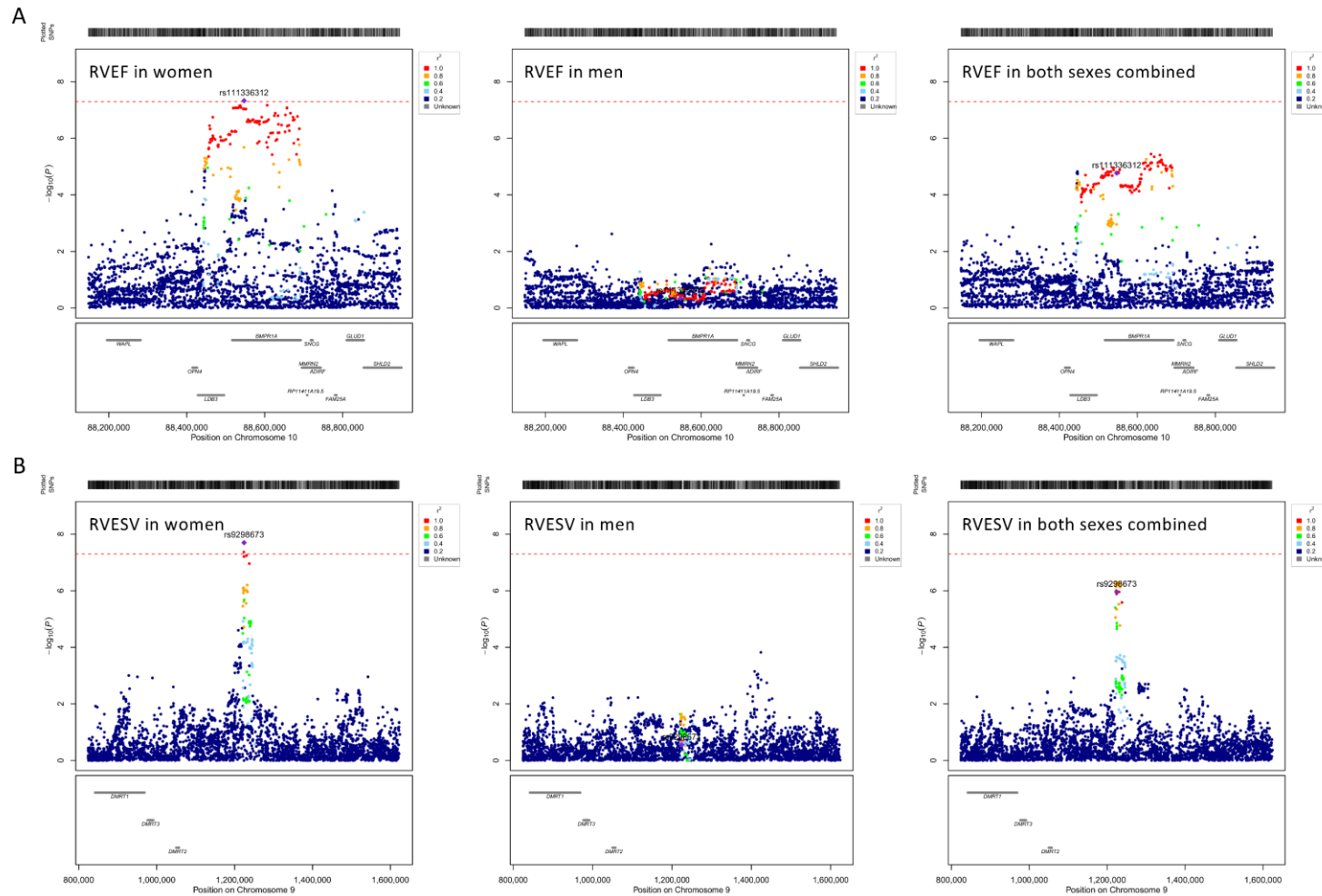


**Figure 2:** Regional association for sex-specific loci.

Regional plots show the genomic positions of variants on the x-axis and their association strength ( $-\log_{10}(p\text{-value})$ ) on the y-axis. Correlation coefficients ( $r^2$ ) with the lead variants are indicated by colour. In **A**, the locus for RVEF on chromosome 10 is displayed. In **B**, the locus for RVESV on chromosome 9.

RV end-systolic volume (RVESV). RV ejection fraction (RVEF).

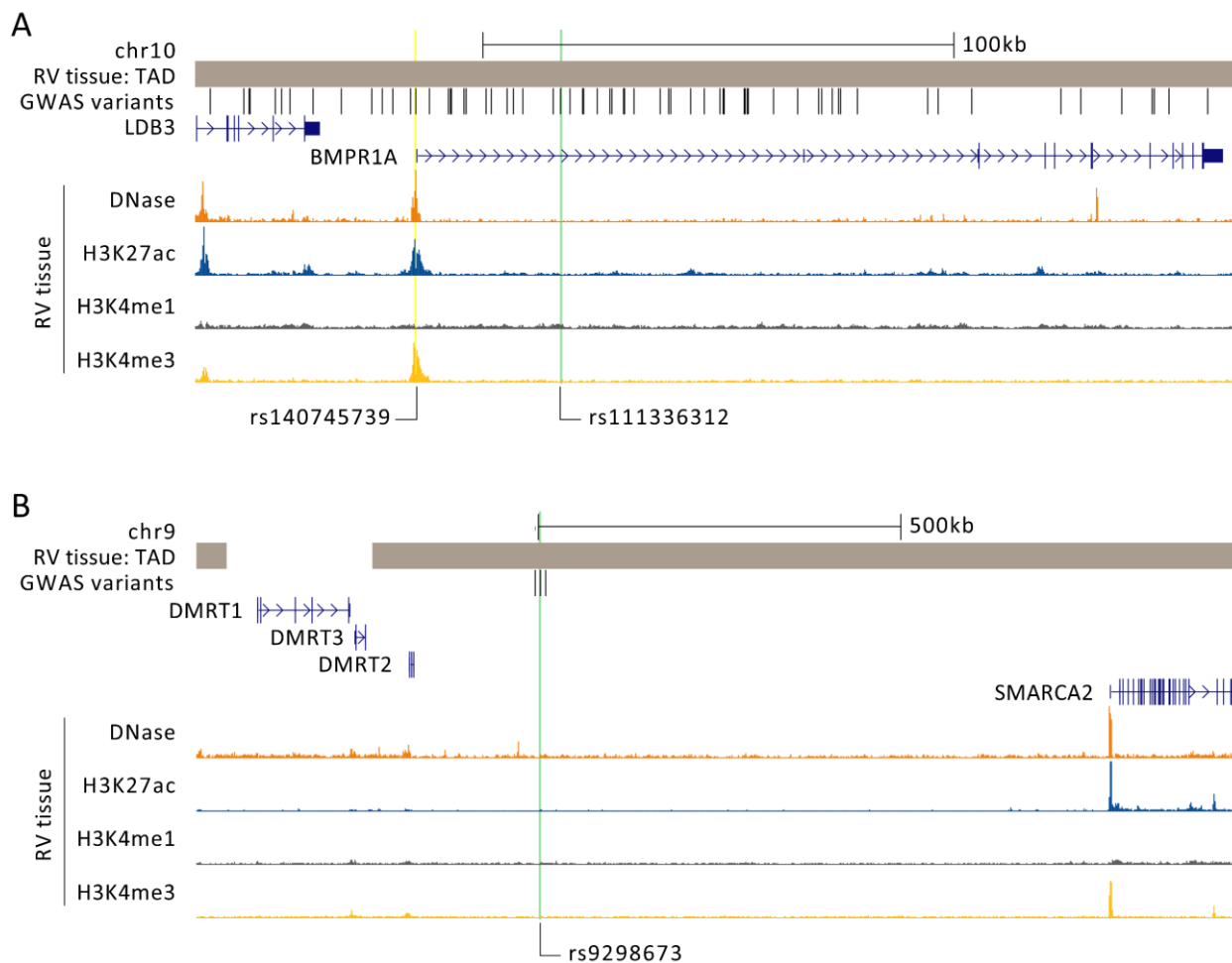


**Figure 3:** Epigenetic marks in right ventricular (RV) tissue from adult women.

Topologically associated domains (TAD) indicate genomic regions that are in close proximity based on the 3-dimensional chromatin structure (Hi-C maps). GWAS variants are displayed that are in high LD with the lead variant ( $r^2 > 0.9$ ). Lead variants are highlighted in green. DNase I hypersensitivity sites mark chromatin regions that are assessable for transcription factors. Epigenomic modification indicate areas likely to contain active regulatory regions and promoters. H3K4Me1 is often found in enhancers, H3K4Me3 typically marks promoters and H3K27ac is often marking active regulatory regions. In **A**, the female-specific locus for RVEF on chromosome 10 is displayed. Here a variant rs140745739 (highlighted in yellow) that is in high LD with lead variant ( $r^2 = 0.97$ ) resides within the active promoter region of BMPR1A. In **B**, the female-specific locus for RVESV on chromosome 9 is displayed. DMRT2 is the closest gene and shares a TAD with the GWAS variants but no adjacent active regulatory region is found.

Bone morphogenetic protein receptor type 1A (BMPR1A). Doublesex and mab3-related transcription factor 1 to 3 (DMRTs). Histone H3 lysine 4 monomethylation (H3K4Me1). Histone H3 lysine 4 trimethylation (H3K4Me3). H3 lysine 27 acetylation (H3K27ac). LIM Domain Binding 3 (LDB3). RV end-systolic volume (RVESV). RV ejection fraction (RVEF). SWI/SNF Related, Matrix Associated, Actin Dependent Regulator Of Chromatin, Subfamily A, Member 2 (SMARCA2).

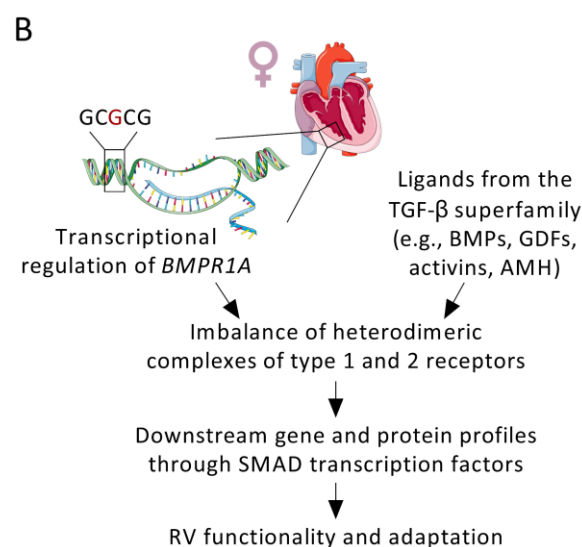
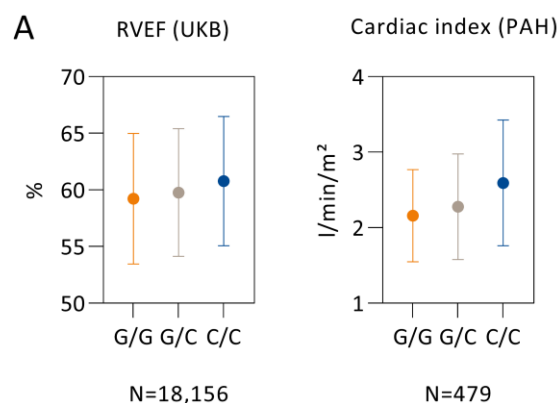


**Figure 4:** *BMPR1A* locus in women.

In **A**, aligned genotypic effects of the *BMPR1A* promoter variant (rs140745739, minor allele C) on right ventricular ejection fraction (RVEF) in 18,156 female participants of the UK Biobank (UKB) and on cardiac index in 479 female patients with idiopathic or hereditary pulmonary arterial hypertension (PAH). Data are presented as the mean with standard deviation. In **B**, a schematic depicts potential mechanisms of *BMPR1A* in RV biology in women.

Anti-Müllerian hormone (AMH). Bone morphogenetic proteins (BMPs). Bone morphogenetic protein receptor type 1A (*BMPR1A*). Growth differentiation factors (GDFs). Transforming growth factor (TGF).